HHS Public Access

Author manuscript

Arterioscler Thromb Vasc Biol. Author manuscript; available in PMC 2021 May 01.

Published in final edited form as:

Arterioscler Thromb Vasc Biol. 2020 May ; 40(5): 1239–1255. doi:10.1161/ATVBAHA.120.314139.

Targeted inhibition of gut microbial TMAO production reduces renal tubulointerstitial fibrosis and functional impairment in a murine model of chronic kidney disease

Nilaksh Gupta[1,2], **Jennifer A. Buffa**[1,2], **Adam B Roberts**[1,2], **Naseer Sangwan**[1,2], **Sarah M. Skye**[1,2], **Lin Li**[1,2], **Karen J. Ho**[4], **John Varga**[5], **Joseph A. DiDonato**[1,2], **W.H. Wilson Tang**[1,2,3], **Stanley L. Hazen**[1,2,3]

[1]Department of Cardiovascular & Metabolic Sciences, Lerner Research Institute; Cleveland Clinic, Cleveland, OH 44195.

[2]Department of Cardiovascular & Metabolic Sciences, Center for Microbiome & Human Health; Cleveland Clinic, Cleveland, OH 44195.

[3]Department of Cardiovascular Medicine, Heart and Vascular Institute; Cleveland Clinic, Cleveland, OH 44195.

[4]Division of Vascular Surgery, Northwestern University Feinberg School of Medicine, Chicago, IL.

[5]Division of Rheumatology, Northwestern University, Chicago, IL.

Abstract

Objective: Gut microbial metabolism of dietary choline, a nutrient abundant in a Western diet, produces trimethylamine (TMA) and the atherothrombosis- and fibrosis-promoting metabolite trimethylamine-N-oxide (TMAO). Recent clinical and animal studies reveal that elevated TMAO levels are associated with heightened risks for both cardiovascular disease (CVD) and incident chronic kidney disease (CKD) development. Despite this, studies focusing on therapeutically targeting gut microbiota-dependent TMAO production and its impact on preserving renal function are limited.

Approach and Results: Herein we examined the impact of pharmacological inhibition of choline diet-induced gut microbiota-dependent production of TMA, and consequently TMAO, on renal tubulointerstitial fibrosis and functional impairment in a model of CKD. Initial studies with a gut microbial choline TMA-lyase mechanism-based inhibitor, iodomethylcholine (IMC), confirmed both marked suppression of TMA generation, and consequently TMAO levels, and selective targeting of the gut microbial compartment (i.e. both accumulation of the drug in intestinal microbes, and limited systemic exposure in the host). Dietary supplementation of either

Address correspondence to: Stanley L Hazen, Department of Cardiovascular & Metabolic Sciences, Lerner Research Institute, 9500 Euclid Ave, mail-code NC-10, Cleveland Clinic, Cleveland, OH 44195.

Disclosures

Dr. Hazen is named as co-inventor on pending and issued patents held by the Cleveland Clinic relating to cardiovascular diagnostics or therapeutics, and reports having the right to receive royalty payment for inventions or discoveries related to cardiovascular diagnostics or therapeutics from Cleveland Heart Laboratory Inc, Quest Diagnostics and Procter & Gamble. Dr. Hazen also reports having been paid as a consultant for Procter & Gamble, and receiving research funds from Astra Zeneca, Procter & Gamble, Pfizer Inc, and Roche Diagnostics. All other authors declared no competing interests.

choline or TMAO significantly augmented multiple indices of renal functional impairment and fibrosis associated with chronic subcutaneous infusion of isoproterenol. However, the presence of the gut microbiota-targeting inhibitor IMC blocked choline diet-induced elevation in TMAO, and both significantly improved decline in renal function, and significantly attenuated multiple indices of tubulointerstitial fibrosis. IMC treatment also reversed many choline diet-induced changes in cecal microbial community composition associated with TMAO and renal functional impairment.

Conclusions: Selective targeting of gut microbiota-dependent TMAO generation may prevent adverse renal structural and functional alterations in subjects at risk for CKD.

Graphical Abstract

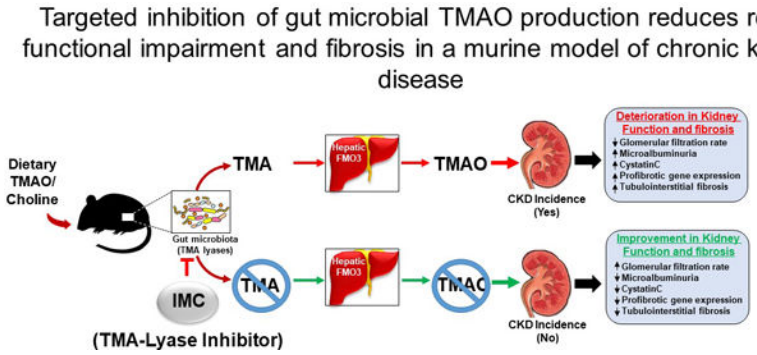

Keywords

Gut microbiome; chronic kidney disease; fibrosis; trimethylamine N-oxide

Introduction

It is becoming increasingly apparent that gut microbiota play a role in both the development of chronic kidney disease (CKD) and its progression to end-stage renal disease (ESRD)[1–5]. The gut microbiome contributes to the generation of metabolites that display uremic toxicity[6–8] and that can potentially contribute directly to the pathophysiology of both CKD and ESRD. For example, gut microbiota-derived uremic toxins have been implicated in CKD progression through promotion of adverse pathophysiologic changes in the kidney, including fibrosis[9], loss of renal tubular function[10,11], and reduction in glomerular filtration rate (GFR)[12]. Despite this growing appreciation, understanding of the direct gut microbiota participants involved is limited, since neither the microbes, nor the specific microbial enzymes and their nephrotoxic products are unambiguously defined. Consequently, therapeutic strategies that limit gut microbiota-dependent contributions to the clinical progression of CKD are limited. Rather, many recent studies in this area have focused on preventing the accumulation of gut microbiome-derived uremic toxins in subjects for whom extensive renal functional decline has already occurred (i.e. ESRD) by adjusting the length and/or types of dialysis in an effort to improve potential toxic metabolite elimination[13,14]. Other recent studies have pursued the use of probiotics to alter microbial composition[15,16], or the use of resins[17] to intercept gut microbial metabolites that are made before systemic adsorption. Unfortunately, most of these treatments display inherent disadvantages,

including adverse side effects, high cost, and notably, they often have sought to reduce levels after the renal functional decline and fibrosis have occurred (e.g. in ESRD). Consequently, the targeting of a gut microbiota pathogenic process for the prevention or treatment of CKD has yet to become adopted into clinical practice.

The meta-organismal production of trimethylamine *N*-oxide (TMAO) has recently emerged as a gut microbiota-dependent metabolite with both clinical and mechanistic links to cardiovascular and metabolic diseases, including CKD. TMAO production begins with nutrient precursors abundant in red meat and a Western diet, such as phospatidylcholine, choline, and carnitine. Gut microbes can utilize these nutrient precursors as a carbon fuel source, generating as a waste product trimethylamine (TMA), which, following absorption into the portal blood, is converted with near first pass kinetics within the liver to TMAO by a family of hepatic flavin monooxygenases (FMOs), particularly FMO_3. Clinical studies have demonstrated that systemic circulating TMAO levels are associated with adverse CVD events (e.g. heart attack, stroke, and death) within multiple cardiovascular and CKD cohorts[1,18,19]. Moreover, numerous animal model studies indicate that microbiota-dependent TMAO generation can directly contribute to the pathogenesis of both atherosclerosis and thrombosis. In these animal studies, a diet supplemented with choline to levels consistent with that observed in omnivorous subjects on a Western diet results in elevation in TMAO to levels observed in humans, and after chronic exposure, was shown to foster both progressive renal functional impairment and enhanced fibrosis[1]. Human subject intervention studies have similarly shown that provision of oral supplementary choline to healthy volunteers substantially increases TMAO levels, with concurrent increases in platelet reactivity to submaximal levels of agonists[20]. In addition, community-based clinical studies such as the Framingham Heart Study (in subjects with normal renal function at baseline), have reported a strong association between high circulating TMAO and choline levels at baseline and incident risk for future development of CKD[21].

Given the potential contribution of gut microbiota-dependent generation of TMAO to both cardiovascular and metabolic diseases, substantial effort has recently been focused on developing approaches to selectively target the meta-organismal TMAO pathway. Toward that end, we have recently developed and characterized use of poorly adsorbed, non-lethal small molecule inhibitors of gut microbiota-dependent conversion of choline → TMA (i.e. choline TMA-lyase activity inhibition) as an effective means of attenuating atherosclerosis[22] and thrombosis[23]. To date, little is known about the potential for therapeutically targeting the TMAO pathway to prevent renal functional impairment and fibrosis in animal models of CKD.

We have recently developed a family of mechanism-based suicide substrate inhibitors designed to be minimally absorbed into the host, but rather, to selectively accumulate within and target gut microbe production of TMA in a non-lethal fashion. Moreover, the new family of inhibitors (halomethylcholines) were shown to be over 10,000 fold more potent (sub-nanomolar IC50) than prior reported microbial choline TMA lyase inhibitors, and to both suppress microbial production of TMA and plasma TMAO levels in the host[23]. Using several members of this family of mechanism-based inhibitors and animal models of thrombosis (carotid artery injury), we showed inhibition of diet-dependent enhancement in

both platelet responsiveness and *in vivo* thrombosis potential, without enhancing bleeding risks[23]. Use of these gut microbe - targeting inhibitors for suppression of renal functional decline and fibrosis in a model of CKD has yet to be reported. Herein we evaluate the impact of iodomethylcholine (IMC), a prototypic mechanism-based gut microbial choline TMA-lyase inhibitor, on choline diet-induced adverse renal structural and functional changes in a chronic sympathetic driven (isoproterenol infusion) model of CKD.

Materials and Methods

The authors declare that all supporting data are available within the article and its online supplementary files.

Experiment design

To avoid the potential nephroprotective effects of estrogen[24–27], only male C57BL/6J mice were used (The Jackson Laboratory, Bar Harbor, ME). Mice were kept on a 12:12 hour light-dark cycle with free access to diet and water. Mice were bred and maintained on Tekled (Envigo) diet 2918 (an irradiated global 18% protein rodent diet). Upon enrollment in studies, mice were initially placed on the indicated diets/groups: (i) Control diet: Teklad (Envigo) 2018 (a global 18% protein rodent diet), a standard normal rodent diet without added choline that in mass spectrometry studies we confirmed contains 0.08gm% total choline content; (ii) TMAO diet: the Control diet supplemented with an additional 0.3gm% TMAO; (iii) Choline diet: the Control diet supplemented with an additional 1gm% choline (i.e. 1.08gm% total choline); and (iv) Choline + IMC diet: the Control diet supplemented with an additional 1gm% choline + 0.06gm% IMC. After one week of diet alone, isoproterenol was subcutaneously infused via mini-osmotic pump (Alzet, Cat#1004, Colorado City, CO, USA) at a concentration of 30mg/kg/day for 28 days, along with continued administration of the indicated diet/intervention arms. All animal model studies were approved by the Institutional Animal Care and Use Committee at the Cleveland Clinic.

To examine intestinal luminal content, animals were humanely euthanized by anesthesia overdose (>300 mg/kg ketamine + 30 mg/kg xylazine), and the small intestine, cecum, and colon were collected. Luminal content was removed and levels of metabolites were quantified as previously described[23]. LC–MS/MS was used to quantify plasma levels of TMAO, TMA, choline, betaine, IMC, and iodomethylbetaine (IMB), and urinary levels of creatinine, as previously described[22,23,28,29]. Their isotope (d9)-labeled analogs were used as internal standards. d2-IMC was synthesized and used as an internal standard for IMC quantification, and d9-betaine was used as an internal standard for IMB quantification, as previously described[23]. LC–MS/MS analyses were performed on a Shimadzu 8050 triple quadrupole mass spectrometer.

Renal function assessment

Transdermal FITC-sinistrin clearance was performed to measure GFR in conscious mice, as previously described[30–32]. The FITC-sinistrin half-life was calculated using a three-compartment model with linear fit using MPD Studio software (MediBeacon, Mannheim, Germany). Cystatin C was measured 4 weeks after isoproterenol exposure using a

commercially available mouse enzyme-linked immunosorbent assay (R&D systems, Minneapolis MN), as previously described[1]. Urinary albumin was measured with a murine microalbuminuria enzyme-linked immunosorbent assay kit (Ethos Biosciences, Cat#1011, Philadelphia, PA) in accordance with manufacturer's protocol.

Renal histology

At time of sacrifice, kidneys were collected, fixed in formalin, and embedded in paraffin. For Picrosirius red staining (PSR), deparafinized 5 μm serial kidney sections were stained with PSR solution [0.5 g direct red (Sigma-Aldrich) dissolved in 500 ml picric acid (Sigma-Aldrich)]. The kidney sections were mounted under a Leica DM 2500 microscope and digitized with a QImaging MicroPublisher 5.0 RTV camera for wide field microscopy. Quantitative morphometric analysis was performed as previously described[1]. Briefly, collagen volume was determined on cortical fields (at least 10 from each animal) lacking major blood vessels using automated (for batch analysis) and customized algorithms/scripts (ImageIQ Inc., Cleveland, OH) written for Image Pro Plus 7.0. Briefly, a set of representative images was chosen that demonstrated a wide range of staining intensities and prevalence. In an automated script, these "training" images were loaded one after another prompting the user to delineate "red" pixels representing positive collagen staining using an interactive color picking tool. An iterative color profile or classifier was generated and subsequently applied to all images in a given directory using a fully automated algorithm. Positive pixels, as defined by the color profile, were segmented and summed to provide positive staining area. Total tissue area was determined by extracting the "saturation" channel, applying a lo-pass filter, and thresholding the result. Any area within the general tissue boundary that was empty (i.e. white) was removed by converting the original image to grayscale and applying a fixed threshold for non-background pixels on adequately white-balanced images. Finally, total tissue area and total stained area were exported to Excel. For post-processing verification, segmented regions were superimposed onto the original image (green outlines) and saved for each image analyzed. For Masson's trichrome staining, slides were deparaffinized, rehydrated, and stained using a commercially available kit for Masson's trichrome staining (Sigma-Aldrich). Five to 10 non-overlapping, high-powered fields from the cortical area of each mouse kidney were graded for fibrotic changes on a scale of 0–3 by two investigators blind to the treatment group.

Immunohistochemistry analysis

Slides were deparaffinized and rehydrated. Antigen retrieval was performed in sodium citrate buffer (pH 6) in a pressurized decloaking chamber at 110°C for 5 minutes. Slides were incubated with the anti-α-SMA primary antibody (rabbit polyclonal antibody, Abcam #ab5694) at a 1:500 (0.4μg/ml) dilution overnight. The biotin-conjugated donkey anti-rabbit secondary antibody (Jackson Immuno #711-065-152) was used at a 1:250 dilution for 1 hour. Staining was developed using an avidin-biotin complex conjugated to HRP and DAB substrate with a reaction time of approximately 10 minutes. Five non-overlapping high-powered fields from the cortical area of each kidney were graded for prevalence of staining on a scale of 0–2 by 2 investigators blind to the treatment group.

RNA extraction, reverse transcription, and quantitative polymerase chain reaction

Explanted kidneys were homogenized in RLT buffer complemented with β-mercaptoethanol using TissueLyser II (Qiagen) at 25 m/s for 2 min (2 rounds). Total mRNA from kidney was extracted with RNA fibrous mini kit (Qiagen) according to the manufacturer's protocol. DNAse digestion was performed using the RNase-free DNAse Set (Qiagen). Total RNA extractions were analyzed for purity and concentration using the NanoDrop 1000 spectrophotometer (Thermo Fisher). RNA samples were diluted to a final concentration of 100 ng/μl, and cDNA was prepared using high capacity cDNA reverse transcription kit (Applied Biosystems). Normalization was to GAPDH gene. Real-time polymerase chain reaction (PCR) with an ABI Prism 7000 sequence detection system (Applied Biosystems), based on TaqMan fluorescence methodology, was used for mRNA quantification. TaqMan probe and primers were purchased as TaqMan gene expression assays-on-demand from Applied Biosystems for glyceraldehyde 3-phosphate dehydrogenase (GAPDH) (Mm99999915_g1), transforming growth factor beta (TGF-β) (Mm01227699_m1), collagen type I, alpha 1 (Coll 1a1) (Mm00801666_g1), tissue inhibitor of metalloproteinase 1 (TIMP1) (Mm01341361_m1), and alpha smooth muscle actin (α-SMA) (Mm00725412_s1). Expression level of each tested gene was analyzed in duplicate for each sample and normalized to the expression of the housekeeping reference gene GAPDH. Gene expression was calculated by using the comparative Ct method, using kidney samples of control-treated mice as calibrator samples.

Cecal microbiota composition analyses

16S rRNA gene sequencing methods were adapted from the methods developed for the NIH-Human Microbiome Project[33]. Briefly, genomic DNA was extracted from mouse ceca using a MoBio Power Soil DNA extraction kit (Omega, Norcross, GA). The 16S rRNA V4 region was amplified and sequenced. Raw 16S amplicon sequence and metadata were demultiplexed using *split_libraries_fastq.py* script implemented *in QIIME1.9.1*[34]. The demultiplexed fastq file was split into sample-specific fastq files using *split_sequence_file_on_sample_ids.py* script from *Qiime1.9.1*[34]. Individual fastq files without non-biological nucleotides were processed using Divisive Amplicon Denoising Algorithm (DADA) pipeline[35]. The output of the dada2 pipeline (feature table of amplicon sequence variants (an ASV table)) was processed for alpha and beta diversity analysis using *phyloseq*[36], and *microbiomeSeq* (http://www.github.com/umerijaz/microbiomeSeq) packages in R. Alpha diversity estimates were measured within group categories using *estimate_richness* function of the *phyloseq* package[36]. Non-multidimensional scaling (NMDS) was performed using Bray-Curtis dissimilarity matrix[37] between groups and visualized by using *ggplot2* package[38]. We assessed the statistical significance ($p < 0.05$) throughout, and whenever necessary adjusted p-values for multiple comparisons according to the Benjamini and Hochberg method to control False Discovery Rate[39] while performing multiple testing on taxa abundance according to sample categories. We performed an analysis of variance (ANOVA) among sample categories while measuring α-diversity using the *plot_anova_diversity* function in *microbiomeSeq* package (http://www.github.com/umerijaz/microbiomeSeq). Permutational multivariate analysis of variance (PERMANOVA) with 999 permutations was performed to test the statistical significance of the NMDS patterns with the *ordination* function of the *microbiomeSeq* package. Linear regression was

performed on taxa abundances against TMAO, GFR, cystatin C, and ACR levels in R[40]. 5,872,030 total reads were generated post-quality filtering, with an average of 167,772 reads per sample. Samples were rarefied to a depth of 102,000 sequences/sample.

Statistical analysis

All experimental data are presented as the mean ± SEM values of biological replicates. The D'Agostino-Pearson test was used to test for normality. Unless otherwise stated in methods, statistical significance among different treatment groups was calculated using nonparametric one-way ANOVA followed by Dunn's post hoc test. Global p-values were calculated using the nonparametric Kruskal-Wallis test. For correlation between plasma TMAO levels and fibrosis indices, p-values were calculated using nonparametric Spearman's correlation. Statistical tests used to compare conditions are also indicated in figure legends. GraphPad PRISM 8.0 and R 3.4.4 (Vienna, Austria, 2018) were used to generate graphs and statistics. A p-value of < 0.05 was considered statistically significant.

Results

The suicide substrate inhibitor iodomethylcholine (IMC) selectively targets gut microbial TMA-lyase activity in the isoproterenol infusion model

In the present study we elected to use chronic isoproterenol infusion as a model of CKD, since it previously has been shown to accelerate renal functional decline and tubulinterstitial fibrosis in animal models[43,47,48]. CKD and end-stage renal disease (ESRD) are often accompanied by sympathetic hyperreactivity, which has been shown to contribute to both progressive renal functional decline and high rate of cardiovascular events in these patients[41–43]. Further, sympathetic (adrenergic) overdrive has been noted even in early stages of renal disease, and which parallels the severity of renal functional decline despite adequate blood pressure control[44]. It is also of interest that sympatho-inhibitory drugs have been shown to have renoprotective effects in subjects independent of blood pressure control, further implicating sympathetic stimulation as a contributor to CKD development in humans[45,46]. While the isoproterenol infusion model thus simulates many features of CKD observed in humans, we felt it prudent to first confirm that our proposed gut microbe-targeting drug, IMC, still selectively targeted the gut microbiome compartment in this model since sympathetic hyper-stimulation has also been shown to induce numerous changes in the gastrointestinal tract including alterations (enhancement) in gastric motility, hypersecretion of mucus production, and enhanced gut leakiness[49–53]. Subcutaneous osmotic mini-pumps containing isoproterenol were therefore placed in several groups of mice (Figure 1) for initial pharmacokinetic studies with IMC. Following several weeks of exposure, mice were sacrificed and both serum and intestinal luminal contents were recovered for mass spectrometry analyses. Notably, IMC accumulated to millimolar (0.7–1.3 mM) levels within the cecum and colon where the majority of gut microbiota reside (Figure 1A), while completely suppressing choline diet-induced production of microbial TMA, and consequently TMAO (Figure 1B,E). While only minimally-detectable levels of choline were present within the intestinal luminal contents in the choline-fed mice, addition of IMC both blocked TMA production (Figure 1B) and resulted in further gut microbiota accumulation of choline, the immediate precursor to TMA (Figure 1C). Intestinal luminal levels of betaine, a

major metabolite of choline, were mostly unaffected (Figure 1D). Interestingly, there was TMAO detected in the lumen within the choline-supplemented mice (presumably either by diffusion from the host or enterohepatic recycling), but the addition of inhibitor (IMC) completely suppressed luminal presence of TMAO in the choline-fed mice (Figure 1E). Finally, the primary metabolite of IMC, iodomethylbetaine (IMB), was also observed within the gut lumen (Figure 1F).

In parallel analyses, we examined plasma levels of IMC and TMAO-related pathway metabolites in all three groups of mice. While both TMA ($p=0.01$ vs. control, Figure 2A) and TMAO ($p=0.04$ vs. control, Figure 2B) were significantly increased in the presence of choline diet, addition of IMC dramatically suppressed the choline diet-induced increases (for TMA $p=0.006$; for TMAO $p=0.001$; Figure 2A,B). In contrast to the gut-lumen contents, where it accumulated to millimolar levels, IMC was virtually undetectable in plasma (Figure 2C). In addition, plasma levels of IMB, the primary metabolite of IMC, were only minimally increased in the presence of the drug (Figure 2D). Plasma levels of choline (Figure 2E) and betaine (Figure 2F), however, were not affected by choline diet or by IMC. These findings show that within the isoproterenol infusion model, IMC potently suppresses gut microbiota-driven formation of TMA, and consequently TMAO, within the gut microbial compartment, despite alterations in intestinal motility previously described for chronic sympathetic stimulation[49–51], while also showing little evidence of systemic exposure within the host.

IMC suppresses choline diet-induced TMA, TMAO, renal functional impairment and injury

In additional studies, the impact of either choline diet-induced increases in gut microbial TMAO generation or IMC treatment on renal function and adverse renal remodeling were examined in the isoproterenol infusion model (Figures 3 and 4). In another group of isoproterenol treated mice, we also examined the effect of direct provision of dietary TMAO (0.3gm %) on renal function. Analysis of plasma from mice in all treatment groups pre- and post- (4 weeks) isoproterenol infusion revealed that, compared to control, both TMAO ($p<0.0001$) and choline diet ($p<0.0001$) feeding significantly increased plasma TMAO levels throughout the isoproterenol infusion period, while the presence of IMC completely suppressed the choline diet-induced increase in plasma TMAO levels ($p<0.0001$ vs. 1% choline, Figure 3 B,C). In parallel studies, mouse renal function was directly assessed by transcutaneous measurement of glomerular filtration rate (GFR), as described under Materials and Methods. Notably, both TMAO ($p=0.03$ vs. control, Figure 4A) and choline diet feeding ($p=0.003$ vs. control, Figure 4A) significantly decreased mouse GFR, 31% and 35% respectively, whereas addition of the gut microbial choline TMA-lyase inhibitor IMC virtually completely prevented the choline diet-induced decrease in GFR ($p=0.006$ vs. 1% choline, and $p=0.83$ vs. control; Figure 4A). In additional studies, plasma levels of Cystatin C, an early marker of renal tubular injury, were examined. Plasma Cystatin C levels were increased by 32% (relative to control) in the mice directly fed supplemental TMAO ($p=0.0006$, Figure 4B), and by 26% (relative to control) in mice placed on the supplemental dietary choline ($p=0.004$, Figure 4B). Notably, addition of IMC markedly attenuated dietary choline-induced increases in plasma Cystatin C ($p=0.02$ vs.1% choline, and $p=0.63$ vs. control; Figure 4B). Urinary albumin-to-creatinine ratio (ACR) also was significantly increased with TMAO ($p=0.005$ vs. control, Figure 4C) and choline diet feeding ($p=0.001$

vs. control, Figure 4C), while provision of IMC completely suppressed the choline diet-induced increase in ACR (p=0.005 vs. 1% choline, and p=0.82 vs. control; Figure 4C). Collectively, these data demonstrate that provision of the gut microbial choline TMA-lyase inhibitor, IMC, both suppressed TMAO levels and completely blocked multiple indices of choline diet-induced renal functional impairment and injury.

The gut microbial choline TMA-lyase inhibitor, IMC, suppresses choline diet-induced renal tubulointerstitial fibrosis

We next quantified the extent of renal tubulointerstitial fibrosis in formalin-fixed samples using two independent approaches. We observed a significant 4-fold increase in picrosirius red staining with conditions associated with higher systemic TMAO (i.e. with either TMAO diet feeding ($p<0.0001$ vs. control) or choline diet ($p<0.0001$ vs. control; Figure 5A,B). In contrast, in the presence of the mechanism-based suicide inhibitor IMC, plasma TMAO levels were suppressed, and a significant reduction in the diet-dependent increase in renal tubulointerstitial fibrosis (p=0.03 vs. 1% choline, Figure 5A,B) was observed. When renal tubulointerstitial fibrosis and collagen deposition were instead quantified by mason trichrome staining, significant increases were again noted with both TMAO ($p<0.0001$ vs. control, Figure 6A,B) and choline supplemented diet groups ($p<0.0001$ vs. control, Figure 6A,B), and addition of IMC significantly attenuated the choline diet-induced renal tubulointerstitial fibrosis (p=0.007 vs. 1% choline, Figure 6A,B). Global analyses across all groups of animals revealed a strong dose-dependent relationship between systemic TMAO levels and extent of renal tubulointerstitial fibrosis, as quantified using either picrosirius red staining ($r=0.76$, $p<0.0001$, Figure 5C) or Masson's trichrome staining ($r=0.73$, $p<0.0001$, Figure 6C). These data thus show that gut microbiota generated TMA(O) provokes renal functional decline and enhanced fibrosis, and that targeted inhibition of microbial choline TMA-lyase activity with an inhibitor that is poorly absorbed by the host, IMC, blocks both the renal functional decline and tubulointerstitial fibrosis observed in this model.

The gut microbiota-targeting choline TMA-lyase inhibitor IMC prevents multiple renal profibrotic gene expression changes

In mRNA analyses, we observed modest but statistically significantly increases in TGF-β gene expression in renal tissues recovered from mice fed the choline-supplemented diet (p=0.01 vs. control, Figure 6A). Moreover, addition of IMC significantly suppressed choline diet-induced increases in TGF-β gene expression ($p<0.0001$ vs. 1% choline, Figure 7A). Similar patterns of profibrotic gene expression changes were observed (increase with choline diet, reversal of choline diet-induced increase with addition of IMC) with several additional pro-fibrotic genes, including the fibrillar collagen gene *col1a1*, the inhibitor of tissue metalloproteinases *timp1*, and alpha smooth muscle actin (α-SMA), a commonly used myofibroblast marker ($p<0.0001$, p=0.008, and p=0.001, respectively, Figure 7B,C,D). Direct provision of TMAO, which resulted in intermediate (more modest) TMAO increases (compared to the choline fed animals), similarly resulted in more modest increases in gene expression levels of the target genes examined, with only some reaching statistical significance (in comparisons with control group; Figure 7).

Gut microbial choline TMA-lyase inhibition attenuates choline diet induced-α-SMA protein expression

We also performed quantitative immunohistochemical staining for protein level of murine α-SMA in renal tissues, as described in Materials and Methods. α-SMA protein tissue staining was significantly increased in mice chronically exposed to higher levels of TMAO, whether it be via direct provision of dietary TMAO ($p<0.0001$ vs. control, Figure 8A,B) or choline-supplemented diet ($p<0.0001$ vs. control, Figure 7A,B). Importantly, provision of the gut microbiota-targeting inhibitor IMC significantly attenuated the choline diet-induced changes, thereby attenuating the extent of α-SMA tissue staining quantified ($p=0.007$ vs. 1% choline, Figure 8A,B). We also noted a significant increase in α-SMA protein among TMAO-fed animals, while α-SMA mRNA expression did not change. We speculate that α-SMactin mRNA expression changes were not persistent through to the time of animal sacrifice despite the chronic (1 month) exposure to elevated circulating TMAO levels and sympathetic hyper-stimulation, whereas protein (and fibrosis) are more persistent (i.e. a difference in lifespan/persistence of RNA vs protein). Consistent with this, rapid and persistent elevations in α-SMA protein independent of RNA transcript abundance have previously been noted[54,55,56]. Notably, when examined across all groups of mice, a strong dose-dependent relationship was observed between systemic (plasma) TMAO levels and quantitation of renal α-SMA protein content ($r=0.75$, $p<0.0001$, Figure 8C).

Gut microbial choline TMA-lyase inhibition reverses many choline diet-induced gut microbiota community changes

In further studies, we examined the impact of dietary choline supplementation and IMC treatment on gut microbial community structure, with a focus on TMAO-associated taxa whose proportions are also linked to measures of renal functional impairment. Cecal microbial DNA encoding 16S ribosomal RNA was sequenced and, in initial analyses, nonmetric multidimensional scaling (NMDS) was performed amongst the 4 groups of mice. Four distinct, non-overlapping clusters were observed (Figure 9A), indicating dietary choline or TMAO supplementation, and dietary choline + IMC exposure, each induced significant (Permanova, $R2=0.49$, $p=0.001$) detectable rearrangements in the overall cecal microbial community. Shannon (which includes evenness) index-based alpha diversity showed significant differences between the different diets (Figure 9B). The control group demonstrated significantly ($p < 0.001$) lower alpha diversity in comparison to the other three diets (i.e. choline, TMAO, and choline + IMC). The addition of IMC to choline treatment significantly reduced the alpha diversity ($p<0.05$), consistent with IMC treatment reversing some of the choline diet - induced community shifts observed. The non-parametric Kruskal-Wallis H-test permitted further identification of three cecal microbial taxa whose proportions accounted for significant ($p< 0.05$, BH-FDR corrected) differences observed in the IMC-treated versus non-IMC-treated groups (Figure 9C).

In further analyses, we examined whether the proportions of any of the detected cecal taxa within all groups of mice were significantly correlated with either plasma TMAO levels or markers of renal function and injury, as determined by direct measure of GFR, cystatin C and ACR (Figure I in the online-only Data Supplement). Notably, cecal microbes recovered from the mice fed a high-choline diet showed a significant ($p = 4.33e-4$) increase in the

proportion of the genus *Lactobacillus*, which further demonstrated positive correlations with TMAO (R^2 = 0.22), ACR (R^2 = 0.14) and cystatin C (R^2 = 0.30), and negative correlations with GFR (R^2 = −0.24, Figure 9C; and Figure I panels A,B,C in the online-only Data Supplement). In addition, both TMAO and Choline diets showed reduced proportions of *Bacteroides* compared to control diet, whereas exposure to IMC reversed the proportion of *Bacteroides* to levels observed in mice fed the control diet (p = 5.38e-4, Figure 9C). Furthermore, increased proportions of *Bacteroides* with IMC showed significant negative correlation with plasma TMAO levels (R^2 = −0.31, p=0.027; Figure 9D) and with renal functional metrics monitored (cystatin C (R^2 = −0.47, p=0.016), ACR (R^2 = −0.39, p=1.42e-3) and positive correlation with GFR (R^2 = 0.17, p=0.0016) (Figure 9D and Figure I, panels A,B,C in the online-only Data Supplement). Moreover, *Lachnospiraceae_UCG-002* showed significant enrichment in the group supplemented with TMAO and the high-choline diet-fed groups (Figure 9C, p = 9.44e-6), which further showed positive associations with both Cystatin C (R^2 = 0.52, p=0.034) and ACR (R^2 = 0.52, p=0.01), and a negative association with GFR (R^2 = −0.22, p=3.79e-3) (Figure I, panels A,B,C in the online-only Data Supplement). Numerous parallel and directionally-relevant correlations between the proportions of *Bacteroides, Lactobacillus*, and *Lachnospiraceae_UCG-002*, and changes in tubulointerstitial fibrosis as monitored via multiple approaches (e.g. staining with mason trichrome, picrosirius red or α-SMA) were also observed (Figure II, panels A,B,C in the online-only Data Supplement).

Discussion

Current treatments to slow progression of CKD and to prevent CKD-related complications on the whole are limited, and our major treatment strategies are preventative, focusing predominantly on anti-hypertensive agents[57,58]. Despite these therapies, outcomes in CKD remain poor. Specifically, CKD progression rates remain high and cardiovascular disease remains the major cause of mortality in this at-risk cohort. The present studies suggest that targeting specific gut microbial pathways may prove beneficial for preservation of renal function, and represent an exciting new opportunity for further investigations. It is notable that the gut microbiota-dependent TMAO pathway represents a common underlying potential pathogenic process in both CKD and CVD alike. And recent studies show targeting this pathway with non-lethal inhibition of gut microbiota generation of TMA can attenuate atherosclerosis[22] and thrombosis[23]. The present studies extend these observations and suggest that targeting gut microbiota-driven TMA generation, and thus TMAO elevation, may potentially protect against concurrent heightened cardiovascular disease risks and progression of renal functional decline in CKD subjects.

Recent studies have also shown that dietary interventions (i.e. avoidance of red meat) can markedly reduce TMAO levels in subjects[59]. The present studies thus further raise the concept of alternative approaches for dietary management of patients with CKD. Dietary interventions in CKD patients are an important part of preventive efforts, and in general have suggested minimizing protein intake, in an effort to minimize nitrogenous waste. The present studies suggest a more targeted approach to selectively reduce TMAO levels, while maintaining protein intake, is worth investigation. Sarcopenia and frailty are commonly observed with more advanced stages of renal disease, conditions where maintaining

adequate caloric intake and dietary protein is otherwise recommended. Interestingly, in a recent dietary intervention study in subjects with normal renal function, chronic change in protein source (e.g. red meat, versus white meat or vegetarian) while maintaining isocaloric diets was shown to substantially impacted TMAO levels through several mechanisms. The red meat-rich diet markedly increased TMAO levels due to enhanced density of TMAO precursors, but also by both eliciting substantial changes in gut microbial community functional output of TMA (enhanced conversion of carnitine into TMAO), and lowering the fractional renal excretion of TMAO[59]. Thus, chronic exposure to a diet rich in red meat led to less efficient TMAO excretion, which was reversed by the white meat and non-meat diets[59]. In alternative recent studies, it was reported that a short-term significant increase in the daily protein allowance was associated with increased circulating TMAO levels[60]. The precise choice of protein source can thus have a significant impact on TMAO production and excretion, and further studies seem warranted to determine if differing sources of dietary protein can significantly impact long term renal function changes in subjects with CKD.

The prevalence of CKD is increasing as the population both ages and becomes increasing obese (thereby increasing the prevalence of diabetes)[61]. Elevated plasma TMAO levels in patients with CKD are associated with higher rates of adverse CVD events and mortality. Moreover, elevated levels of both TMAO and choline are associated with enhanced progressive loss of renal function and development of CKD[1,18,19,21,62–64]. It should also be noted, however, that not all published clinical studies on TMAO have reported a significant positive association with CVD risks. While adverse prognostic value for TMAO is observed in many CKD cohorts[1,18,19,62–65], in maintenance hemodialysis populations the incremental prognostic value of TMAO has at times not been clearly demonstrated, suggesting either the smaller size of some of these studies, or a possible plateau effect maybe observed when virtually all members of the cohort examined have high TMAO level (i.e. even the lowest quartile have markedly elevated TMAO levels and further increases in risk may not be observed with further elevations in TMAO)[14,66–68]. There have been multiple recent meta-analyses that have extensively examined the clinical association between TMAO and both incident CVD risks and mortality – all of the published meta-analyses thus far report a significant positive association with increasing TMAO levels independent of traditional CVD risk factors and renal status[62,69,70]. In one meta-analysis, each 10 μM change in TMAO level was associated with an approximate 7.4% increase in mortality rate[62]. It is also notable that a recent clinical investigation in subjects with ESRD on maintenance hemodialysis report that TMAO has a smaller volume of distribution than urea and is cleared better than urea by the kidney. In addition to its dialyzability compared to other more tightly protein bound uremic toxins, this has led to the suggestion that additional strategies in ESRD, such as reducing production coupled with more frequent dialysis, might also help to reduce TMAO levels in ESRD subjects[71].

It is also notable that the present small molecule inhibitor used, IMC, was specifically developed to be non-lethal (i.e. unlike an antibiotic), and thus should exert less selective pressure for development of gut microbial resistance. Moreover, the capacity of the inhibitor to accumulate within gut microbiota *in vivo* was previously developed based on the recognition that upon inhibiting catalysis of choline within the microbe, the bacterial cytosolic levels will accumulate, be sensed as an abundant carbon fuel source, and the entire

cutC gene cluster[72,73], including the bacterial choline transporter[23], could then be upregulated. Thus, the more effective the inhibitor is at blocking choline catabolism, the greater the microbe accumulates both IMC and choline (both of which were noted in the present studies to be highly enriched within the gut luminal contents, which are predominantly comprised of gut bacteria). This has the functional outcome of sequestering choline from the gut luminal extracellular space, depriving other microbial community members from choline. Thus, as long as a significant enough proportion of microbes within the community are sufficiently inhibited, depletion of intestinal luminal choline will suppress colon gut microbial community output of TMA (and thus host production of TMAO), a process that would be more resilient to development of resistance.

The present studies add to the growing body of evidence mechanistically linking gut microbiota-generated TMA/TMAO to multiple indices of renal functional impairment and fibrosis. They also suggest that further studies exploring the link between TMAO levels and risk for glomerular and tubular injury in subjects are needed. Renal fibrosis, a consequence of an excessive accumulation of extracellular matrix, represents a relatively late and common manifestation of nearly all chronic and progressive nephropathies[58]. It is thus of interest that elevated gut microbiota-driven plasma TMAO levels appear to directly contribute to enhanced fibrosis in this mouse model, where multiple different indices of fibrosis were quantitatively examined (i.e. histological staining procedures and pro-fibrotic gene expression changes, protein levels). Whether non-lethal gut microbiota-targeting inhibitors that suppress TMAO levels represent a new renal-sparing therapy in some subjects with CKD awaits further investigation.

Several limitations of the present study warrant consideration. Most notably, not all CKD will be driven by TMAO-dependent mechanisms. While CKD is associated with elevated TMAO levels, not all subjects with CKD have elevated TMAO. Thus, one could imagine a gut microbe-targeted TMA lyase inhibitor to be used with the companion diagnostic TMAO test, as inhibition of this pathway would be more likely to show benefit amongst subjects with heightened TMAO levels. In addition, the effect of reducing TMAO on CKD progression rate in humans remains to be evaluated. Moreover, while the present studies have demonstrated that inhibiting TMAO production can prevent both renal functional impairment and fibrosis, they have not examined if reduction in TMAO with established renal disease can either halt the progression of, or foster regression in, renal functional decline and adverse remodeling. Finally, beyond the induction of multiple pro-fibrotic gene expression changes, the present studies do not examine the molecular mechanisms by which TMAO exerts its adverse effects on renal functional impairment and fibrosis. Notably, a recent study by Biddinger and colleagues reported the discovery of the endoplasmic reticulum stress kinase PERK (EIF2AK3) as a TMAO receptor for glucose-related metabolic effects associated with the metabolite[74]. It remains unknown if PERK participates in TMAO-driven renal function decline or if TMAO is acting via other proposed mechanisms, such as an alternate (still un-identified) receptor, or via demonstrated effect on protein conformation and stability[75,76].

In conclusion, the present studies provide further evidence in support of a gut microbial contribution to renal function decline and adverse remodeling in a chronic sympathetic-

driven isoproterenol infusion model of CKD. More significantly, the results indicate that targeting TMAO metabolism may represent a potential therapeutic approach for preventing or retarding CKD development and progression, while concurrently reducing adverse cardiovascular events associated with TMAO elevation. Moving beyond TMAO, one can also envision multiple potential gut microbiota-generated uremic toxins[77] as potential additional candidates for therapeutic intervention and investigation.

Supplementary Material

Refer to Web version on PubMed Central for supplementary material.

Acknowledgements

N.G. designed, performed, and analyzed data from most of the studies. N.G. also wrote the manuscript with input from all authors. J.A.B. and A.B.R. performed experiments for the luminal detection of IMC and other metabolites in mice, A.B.R performed the mass spec analysis, N.S. and S.M.S. performed microbe composition analyses, and K.J.H. and J.V. performed mason trichrome staining and alpha-SMA staining. L.L. helped with statistical analysis. J.A.D. and W.T. provided critical scientific input and discussions. S.L.H conceived, designed, and supervised all studies, and participated in the drafting and editing of the manuscript. All authors contributed to the critical review of the manuscript.

Sources of Funding

This work received funding from National Institutes of Health and Office of Dietary Supplements grants HL103866, 1P01 HL147823, HL126827 and DK106000, and the Leducq Foundation.

Non-Standard Abbreviations & Acronyms

TMAO	Trimethylamine N-oxide
TMA	Trimethylamine
IMC	Iodomethylcholine
α-SMA	Alpha-Smooth muscle actin

References

1. Tang WH, Wang Z, Kennedy DJ, et al. Gut microbiota-dependent trimethylamine N-oxide (TMAO) pathway contributes to both development of renal insufficiency and mortality risk in chronic kidney disease. Circ Res. 2015;116:448–455. [PubMed: 25599331]
2. Wong J, Piceno YM, DeSantis TZ, Pahl M, Andersen GL, Vaziri ND. Expansion of urease- and uricase-containing, indole- and p-cresol-forming and contraction of short-chain fatty acid-producing intestinal microbiota in ESRD. Am J Nephrol. 2014;39:230–237. [PubMed: 24643131]
3. Strid H, Simren M, Stotzer PO, Ringstrom G, Abrahamsson H, Bjornsson ES. Patients with chronic renal failure have abnormal small intestinal motility and a high prevalence of small intestinal bacterial overgrowth. Digestion. 2003;67:129–137. [PubMed: 12853724]
4. Vaziri ND, Wong J, Pahl M, et al. Chronic kidney disease alters intestinal microbial flora. Kidney Int. 2013;83:308–315. [PubMed: 22992469]
5. Simenhoff ML, Saukkonen JJ, Burke JF, Wesson LG, Schaedler RW. Amine metabolism and the small bowel in uraemia. Lancet. 1976;2:818–821. [PubMed: 61496]
6. Barrios C, Beaumont M, Pallister T, et al. Gut-Microbiota-Metabolite Axis in Early Renal Function Decline. PLoS One. 2015;10:e0134311. [PubMed: 26241311]

7. Kikuchi M, Ueno M, Itoh Y, Suda W, Hattori M. Uremic Toxin-Producing Gut Microbiota in Rats with Chronic Kidney Disease. Nephron. 2017;135:51–60. [PubMed: 27701177]
8. Mishima E, Fukuda S, Mukawa C, et al. Evaluation of the impact of gut microbiota on uremic solute accumulation by a CE-TOFMS-based metabolomics approach. Kidney Int. 2017;92:634–645. [PubMed: 28396122]
9. Sun CY, Chang SC, Wu MS. Uremic toxins induce kidney fibrosis by activating intrarenal renin-angiotensin-aldosterone system associated epithelial-to-mesenchymal transition. PLoS One. 2012;7:e34026. [PubMed: 22479508]
10. Watanabe H, Miyamoto Y, Honda D, et al. p-Cresyl sulfate causes renal tubular cell damage by inducing oxidative stress by activation of NADPH oxidase. Kidney Int. 2013;83:582–592. [PubMed: 23325087]
11. Sun CY, Chang SC, Wu MS. Suppression of Klotho expression by protein-bound uremic toxins is associated with increased DNA methyltransferase expression and DNA hypermethylation. Kidney Int. 2012;81:640–650. [PubMed: 22237753]
12. Meijers BK, Claes K, Bammens B, et al. p-Cresol and cardiovascular risk in mild-to-moderate kidney disease. Clin J Am Soc Nephrol. 2010;5:1182–1189. [PubMed: 20430946]
13. Basile C, Libutti P, Di Turo AL, et al. Removal of uraemic retention solutes in standard bicarbonate haemodialysis and long-hour slow-flow bicarbonate haemodialysis. Nephrol Dial Transplant. 2011;26:1296–1303. [PubMed: 20813765]
14. Kalim S, Wald R, Yan AT, et al. Extended Duration Nocturnal Hemodialysis and Changes in Plasma Metabolite Profiles. Clin J Am Soc Nephrol. 2018;13:436–444. [PubMed: 29444900]
15. Wang IK, Wu YY, Yang YF, et al. The effect of probiotics on serum levels of cytokine and endotoxin in peritoneal dialysis patients: a randomised, double-blind, placebo-controlled trial. Benef Microbes. 2015;6:423–430. [PubMed: 25609654]
16. Viramontes-Horner D, Marquez-Sandoval F, Martin-del-Campo F, et al. Effect of a symbiotic gel (Lactobacillus acidophilus + Bifidobacterium lactis + inulin) on presence and severity of gastrointestinal symptoms in hemodialysis patients. J Ren Nutr. 2015;25:284–291. [PubMed: 25455039]
17. Weir MR, Bakris GL, Bushinsky DA, et al. Patiromer in patients with kidney disease and hyperkalemia receiving RAAS inhibitors. N Engl J Med. 2015;372:211–221. [PubMed: 25415805]
18. Kim RB, Morse BL, Djurdjev O, et al. Advanced chronic kidney disease populations have elevated trimethylamine N-oxide levels associated with increased cardiovascular events. Kidney Int. 2016;89:1144–1152. [PubMed: 27083288]
19. Missailidis C, Hallqvist J, Qureshi AR, et al. Serum Trimethylamine-N-Oxide Is Strongly Related to Renal Function and Predicts Outcome in Chronic Kidney Disease. PLoS One. 2016;11:e0141738. [PubMed: 26751065]
20. Zhu W, Wang Z, Tang WHW, Hazen SL. Gut Microbe-Generated Trimethylamine N-Oxide From Dietary Choline Is Prothrombotic in Subjects. Circulation. 2017;135:1671–1673. [PubMed: 28438808]
21. Rhee EP, Clish CB, Ghorbani A, et al. A combined epidemiologic and metabolomic approach improves CKD prediction. J Am Soc Nephrol. 2013;24:1330–1338. [PubMed: 23687356]
22. Wang Z, Roberts AB, Buffa JA, et al. Non-lethal Inhibition of Gut Microbial Trimethylamine Production for the Treatment of Atherosclerosis. Cell. 2015;163:1585–1595. [PubMed: 26687352]
23. Roberts AB, Gu X, Buffa JA, et al. Development of a gut microbe-targeted nonlethal therapeutic to inhibit thrombosis potential. Nat Med. 2018;24:1407–1417. [PubMed: 30082863]
24. Dubey RK, Gillespie DG, Keller PJ, Imthurn B, Zacharia LC, Jackson EK. Role of methoxyestradiols in the growth inhibitory effects of estradiol on human glomerular mesangial cells. Hypertension. 2002;39:418–424. [PubMed: 11882583]
25. Matsuda T, Yamamoto T, Muraguchi A, Saatcioglu F. Cross-talk between transforming growth factor-beta and estrogen receptor signaling through Smad3. J Biol Chem. 2001;276:42908–42914. [PubMed: 11555647]
26. Mankhey RW, Bhatti F, Maric C. 17beta-Estradiol replacement improves renal function and pathology associated with diabetic nephropathy. Am J Physiol Renal Physiol. 2005;288:F399–405. [PubMed: 15454392]

27. Long DA, Kolatsi-Joannou M, Price KL, et al. Albuminuria is associated with too few glomeruli and too much testosterone. Kidney Int. 2013;83:1118–1129. [PubMed: 23447063]
28. Wang Z, Klipfell E, Bennett BJ, et al. Gut flora metabolism of phosphatidylcholine promotes cardiovascular disease. Nature. 2011;472:57–63. [PubMed: 21475195]
29. Wang Z, Levison BS, Hazen JE, Donahue L, Li XM, Hazen SL. Measurement of trimethylamine-N-oxide by stable isotope dilution liquid chromatography tandem mass spectrometry. Anal Biochem. 2014;455:35–40. [PubMed: 24704102]
30. Scarfe L, Schock-Kusch D, Ressel L, et al. Transdermal Measurement of Glomerular Filtration Rate in Mice. J Vis Exp. 2018.
31. Schreiber A, Shulhevich Y, Geraci S, et al. Transcutaneous measurement of renal function in conscious mice. Am J Physiol Renal Physiol. 2012;303:F783–788. [PubMed: 22696603]
32. Schock-Kusch D, Xie Q, Shulhevich Y, et al. Transcutaneous assessment of renal function in conscious rats with a device for measuring FITC-sinistrin disappearance curves. Kidney Int. 2011;79:1254–1258. [PubMed: 21368744]
33. Human Microbiome Project C Structure, function and diversity of the healthy human microbiome. Nature. 2012;486:207–214. [PubMed: 22699609]
34. Caporaso JG, Kuczynski J, Stombaugh J, et al. QIIME allows analysis of high-throughput community sequencing data. Nat Methods. 2010;7:335–336. [PubMed: 20383131]
35. Callahan BJ, McMurdie PJ, Rosen MJ, Han AW, Johnson AJ, Holmes SP. DADA2: High-resolution sample inference from Illumina amplicon data. Nature methods. 2016;13:581–583. [PubMed: 27214047]
36. McMurdie PJ, Holmes S. phyloseq: an R package for reproducible interactive analysis and graphics of microbiome census data. PloS one. 2013;8:e61217. [PubMed: 23630581]
37. McMurdie PJ, Holmes S. Waste not, want not: why rarefying microbiome data is inadmissible. PLoS computational biology. 2014;10:e1003531. [PubMed: 24699258]
38. Wickham H ggplot2: Elegant Graphics for Data Analysis. Springer Publishing Company, Incorporated; 2009.
39. Benjamini Y Discovering the false discovery rate. Journal of the Royal Statistical Society: Series B (Statistical Methodology). 2010;72:405–416.
40. Tiit E-M. Nonparametric Statistical Methods. Myles Hollander and Douglas A. Wolfe, Wiley, Chichester, 1999. ISBN 0–471-19045-4. Statistics in Medicine. 2000;19:1386–1388.
41. Schlaich MP, Socratous F, Hennebry S, et al. Sympathetic activation in chronic renal failure. J Am Soc Nephrol. 2009;20:933–939. [PubMed: 18799718]
42. Zoccali C, Mallamaci F, Parlongo S, et al. Plasma norepinephrine predicts survival and incident cardiovascular events in patients with end-stage renal disease. Circulation. 2002;105:1354–1359. [PubMed: 11901048]
43. de Ponte MC, Casare FAM, Costa-Pessoa JM, et al. The Role of beta-Adrenergic Overstimulation in the Early Stages of Renal Injury. Kidney Blood Press Res. 2017;42:1277–1289. [PubMed: 29262407]
44. Grassi G, Quarti-Trevano F, Seravalle G, et al. Early sympathetic activation in the initial clinical stages of chronic renal failure. Hypertension. 2011;57:846–851. [PubMed: 21300663]
45. Amann K, Rump LC, Simonaviciene A, et al. Effects of low dose sympathetic inhibition on glomerulosclerosis and albuminuria in subtotally nephrectomized rats. J Am Soc Nephrol. 2000;11:1469–1478. [PubMed: 10906160]
46. Vonend O, Marsalek P, Russ H, Wulkow R, Oberhauser V, Rump LC. Moxonidine treatment of hypertensive patients with advanced renal failure. J Hypertens. 2003;21:1709–1717. [PubMed: 12923404]
47. Zheng G, Cai J, Chen X, et al. Relaxin Ameliorates Renal Fibrosis and Expression of Endothelial Cell Transition Markers in Rats of Isoproterenol-Induced Heart Failure. Biol Pharm Bull. 2017;40:960–966. [PubMed: 28674260]
48. Liu Q, Zhang Q, Wang K, et al. Renal Denervation Findings on Cardiac and Renal Fibrosis in Rats with Isoproterenol Induced Cardiomyopathy. Sci Rep. 2015;5:18582. [PubMed: 26689945]

49. Ide S, Yamamoto R, Takeda H, Minami M. Bidirectional brain-gut interactions: Involvement of noradrenergic transmission within the ventral part of the bed nucleus of the stria terminalis. Neuropsychopharmacol Rep. 2018;38:37–43. [PubMed: 30106262]
50. Thollander M, Svensson TH, Hellstrom PM. Stimulation of beta-adrenoceptors with isoprenaline inhibits small intestinal activity fronts and induces a postprandial-like motility pattern in humans. Gut. 1997;40:376–380. [PubMed: 9135528]
51. Morris AI, Turnberg LA. Influence of isoproterenol and propranolol on human intestinal transport in vivo. Gastroenterology. 1981;81:1076–1079. [PubMed: 6116643]
52. Gati T, Gelencser F, Hideg J. The role of adrenergic receptors in the regulation of gastric motility in the rat. Z Exp Chir. 1975;8:179–184. [PubMed: 44929]
53. Sorribas M, de Gottardi A, Moghadamrad S, et al. Isoproterenol Disrupts Intestinal Barriers Activating Gut-Liver-Axis: Effects on Intestinal Mucus and Vascular Barrier as Entry Sites. Digestion. 2019:1–13.
54. Chothani S, Schafer S, Adami E, et al. Widespread Translational Control of Fibrosis in the Human Heart by RNA-Binding Proteins. Circulation. 2019;140:937–951. [PubMed: 31284728]
55. Zhang A, Liu X, Cogan JG, et al. YB-1 coordinates vascular smooth muscle alpha-actin gene activation by transforming growth factor beta1 and thrombin during differentiation of human pulmonary myofibroblasts. Mol Biol Cell. 2005;16:4931–4940. [PubMed: 16093352]
56. Strauch AR, Hariharan S. Dynamic Interplay of Smooth Muscle alpha-Actin Gene-Regulatory Proteins Reflects the Biological Complexity of Myofibroblast Differentiation. Biology (Basel). 2013;2:555–586. [PubMed: 24832798]
57. National Kidney F KDOQI Clinical Practice Guideline for Diabetes and CKD: 2012 Update. Am J Kidney Dis. 2012;60:850–886. [PubMed: 23067652]
58. Humphreys BD. Mechanisms of Renal Fibrosis. Annu Rev Physiol. 2018;80:309–326. [PubMed: 29068765]
59. Wang Z, Bergeron N, Levison BS, et al. Impact of chronic dietary red meat, white meat, or non-meat protein on trimethylamine N-oxide metabolism and renal excretion in healthy men and women. Eur Heart J. 2019;40:583–594. [PubMed: 30535398]
60. Mitchell SM, Milan AM, Mitchell CJ, et al. Protein Intake at Twice the RDA in Older Men Increases Circulatory Concentrations of the Microbiome Metabolite Trimethylamine-N-Oxide (TMAO). Nutrients. 2019;11.
61. Coresh J, Astor BC, Greene T, Eknoyan G, Levey AS. Prevalence of chronic kidney disease and decreased kidney function in the adult US population: Third National Health and Nutrition Examination Survey. Am J Kidney Dis. 2003;41:1–12.
62. Schiattarella GG, Sannino A, Toscano E, et al. Gut microbe-generated metabolite trimethylamine-N-oxide as cardiovascular risk biomarker: a systematic review and dose-response meta-analysis. Eur Heart J. 2017;38:2948–2956. [PubMed: 29020409]
63. Stubbs JR, House JA, Ocque AJ, et al. Serum Trimethylamine-N-Oxide is Elevated in CKD and Correlates with Coronary Atherosclerosis Burden. J Am Soc Nephrol. 2016;27:305–313. [PubMed: 26229137]
64. Robinson-Cohen C, Newitt R, Shen DD, et al. Association of FMO3 Variants and Trimethylamine N-Oxide Concentration, Disease Progression, and Mortality in CKD Patients. PLoS One. 2016;11:e0161074. [PubMed: 27513517]
65. Gruppen EG, Garcia E, Connelly MA, et al. TMAO is Associated with Mortality: Impact of Modestly Impaired Renal Function. Sci Rep. 2017;7:13781. [PubMed: 29061990]
66. Kaysen GA, Johansen KL, Chertow GM, et al. Associations of Trimethylamine N-Oxide With Nutritional and Inflammatory Biomarkers and Cardiovascular Outcomes in Patients New to Dialysis. J Ren Nutr. 2015;25:351–356. [PubMed: 25802017]
67. Stubbs JR, Stedman MR, Liu S, et al. Trimethylamine N-Oxide and Cardiovascular Outcomes in Patients with End-stage Kidney Disease Receiving Maintenance Hemodialysis. Clin J Am Soc Nephrol. 2019.
68. Shafi T, Powe NR, Meyer TW, et al. Trimethylamine N-Oxide and Cardiovascular Events in Hemodialysis Patients. J Am Soc Nephrol. 2017;28:321–331. [PubMed: 27436853]

69. Heianza Y, Ma W, Manson JE, Rexrode KM, Qi L. Gut Microbiota Metabolites and Risk of Major Adverse Cardiovascular Disease Events and Death: A Systematic Review and Meta-Analysis of Prospective Studies. J Am Heart Assoc. 2017;6.

70. Qi J, You T, Li J, et al. Circulating trimethylamine N-oxide and the risk of cardiovascular diseases: a systematic review and meta-analysis of 11 prospective cohort studies. J Cell Mol Med. 2018;22:185–194. [PubMed: 28782886]

71. Hai X, Landeras V, Dobre MA, DeOreo P, Meyer TW, Hostetter TH. Mechanism of Prominent Trimethylamine Oxide (TMAO) Accumulation in Hemodialysis Patients. PLoS One. 2015;10:e0143731. [PubMed: 26650937]

72. Osbourn AE, Field B. Operons. Cell Mol Life Sci. 2009;66:3755–3775. [PubMed: 19662496]

73. Craciun S, Balskus EP. Microbial conversion of choline to trimethylamine requires a glycyl radical enzyme. Proc Natl Acad Sci U S A. 2012;109:21307–21312. [PubMed: 23151509]

74. Chen S, Henderson A, Petriello MC, et al. Trimethylamine N-Oxide Binds and Activates PERK to Promote Metabolic Dysfunction. Cell Metab. 2019;30:1141–1151 e1145. [PubMed: 31543404]

75. Seldin MM, Meng Y, Qi H, et al. Trimethylamine N-Oxide Promotes Vascular Inflammation Through Signaling of Mitogen-Activated Protein Kinase and Nuclear Factor-kappaB. J Am Heart Assoc. 2016;5.

76. Moore JO, Hendrickson WA. Structural analysis of sensor domains from the TMAO-responsive histidine kinase receptor TorS. Structure. 2009;17:1195–1204. [PubMed: 19748340]

77. Devlin AS, Marcobal A, Dodd D, et al. Modulation of a Circulating Uremic Solute via Rational Genetic Manipulation of the Gut Microbiota. Cell Host Microbe. 2016;20:709–715. [PubMed: 27916477]

Highlights

1. The suicide substrate inhibitor iodomethylcholine (IMC), which is nonlethal to gut microbes, selectively targets gut microbial TMA lyase activity and suppresses choline diet induced TMA, TMAO, renal functional impairment [glomerular filtration rate (GFR) and Cystatin C] and injury (albumin to creatinine ratio).
2. The gut microbial choline TMA-lyase inhibitor, IMC, suppresses choline-diet-induced renal tubulointerstitial fibrosis and profibrotic gene expression.
3. The present studies reveal a novel approach that targets the gut microbial TMAO pathway and both prevents renal functional decline and tubulointerstitial fibrosis *in vivo*, while simultaneously limiting systemic exposure and potential for adverse side effects in the host.

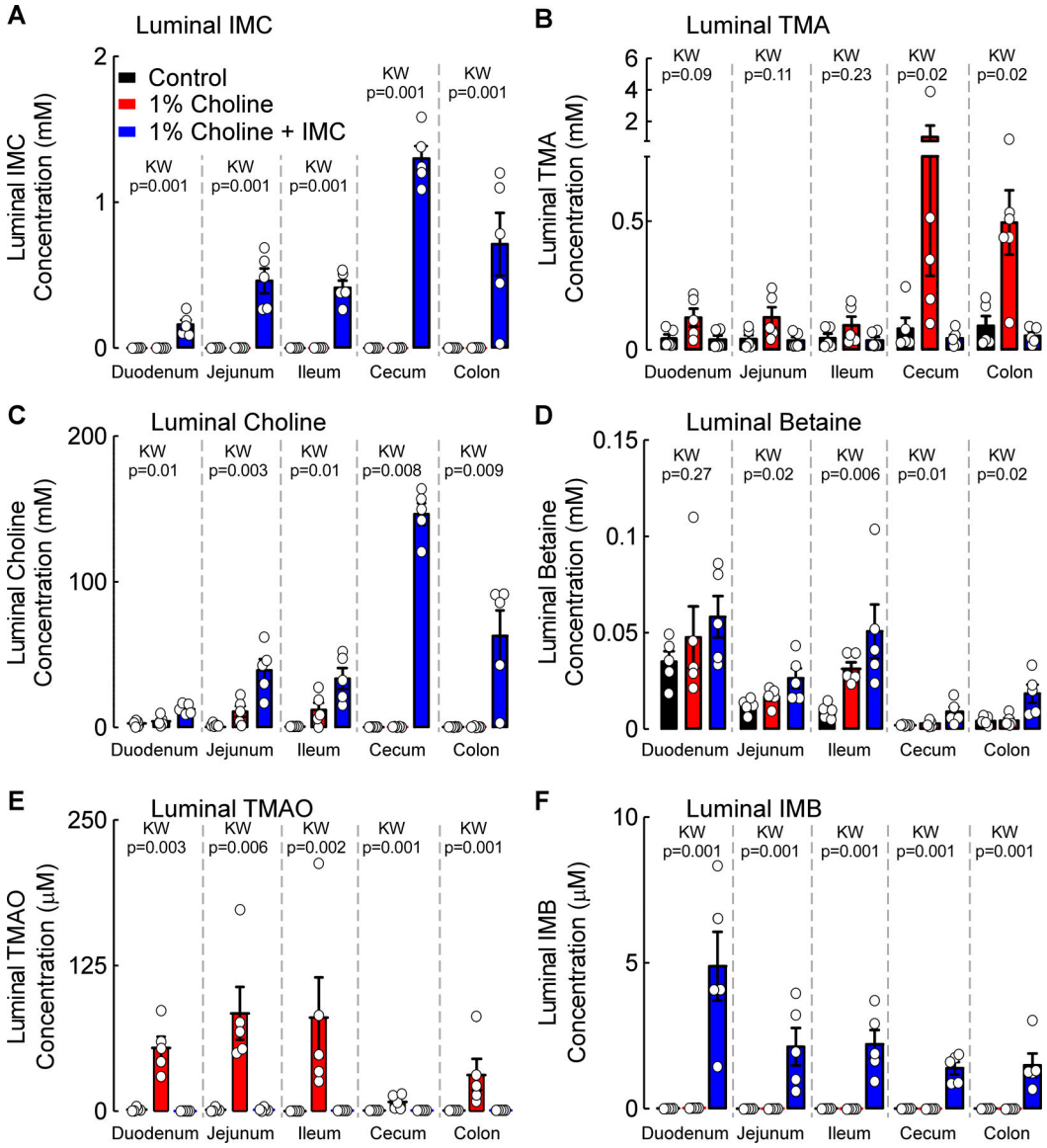

Figure 1. Microbial TMA-lyase inhibitor, IMC, selectively accumulates within the gut microbial compartments.

Luminal concentrations of **(A)** Iodomethylcholine (IMC), **(B)** Trimethylamine (TMA), **(C)** Choline, **(D)** Betaine, **(E)** Trimethylamine *N*-oxide (TMAO), and **(F)** Iodomethylbetaine (IMB). Results represent the mean ± SEM (n=5) and global p-value for each luminal segment was obtained by nonparametric Kruskal-Wallis (KW) test.

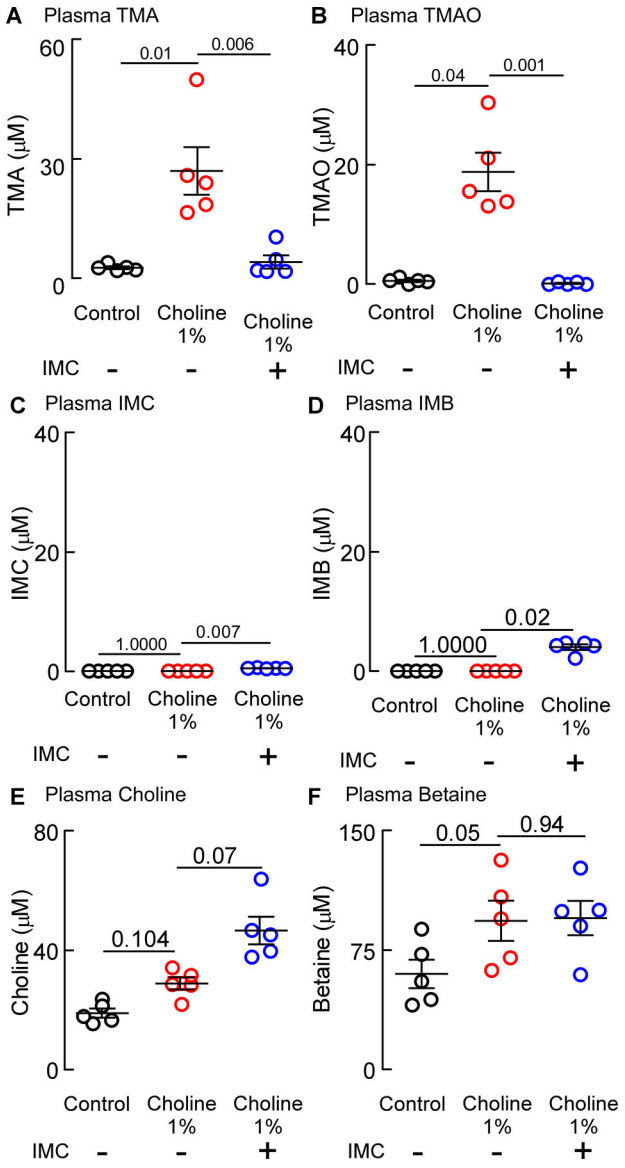

Figure 2. Microbial TMA-lyase inhibitor IMC significantly reduces gut-microbe dependent plasma TMA and TMAO levels.

Plasma concentrations of **(A)** Trimethylamine (TMA), **(B)** Trimethylamine N-oxide (TMAO), **(C)** Iodomethylcholine (IMB), **(D)** Iodomethylbetaine (IMB), **(E)** Choline, and **(F)** Betaine. Results represent the mean ± SEM (n=5) and the p-value among different treatments was determined by nonparametric 1-way ANOVA after Dunn's post hoc test.

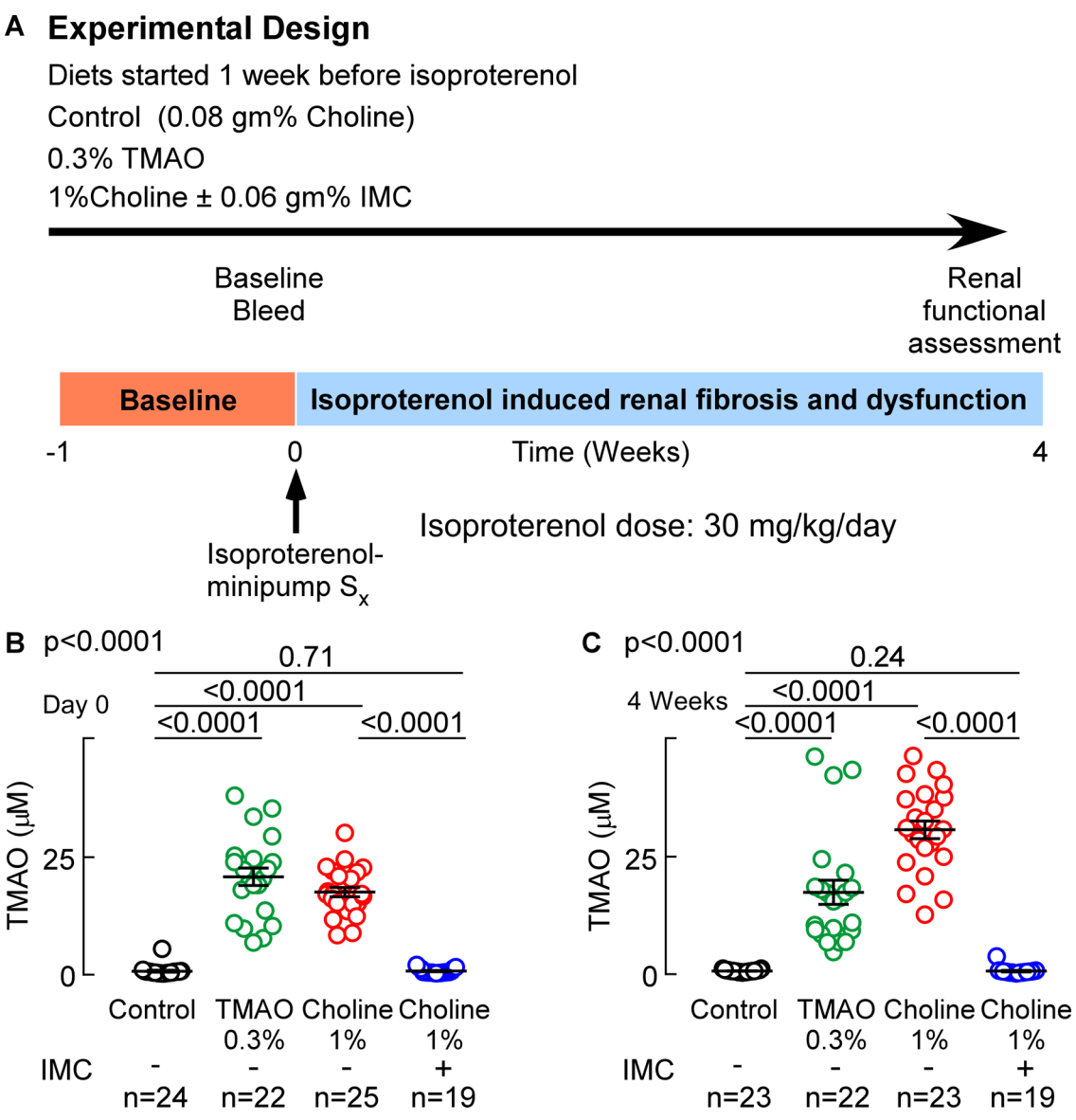

Figure 3. Choline TMA-lyase inhibitor, IMC, suppresses gut-microbe dependent plasma TMAO levels.

(A) Wild-type C57BL/6J male mice (10 weeks old) were fed indicated diets for 7 days. After 7 days, isoproterenol (30 mg/kg BW/day, 28 days) was infused subcutaneously with vehicle, via osmotic mini-pumps along with the indicated diets for 4 weeks. Mice were humanely sacrificed at the end of the study and kidneys were dissected and frozen in liquid nitrogen (for protein or mRNA extraction) and fixed in 4% buffered formaldehyde (for histology and immunohistochemistry). **(B)** Plasma Trimethylamine *N*-oxide (TMAO) levels at day 0 (before isoproterenol infusion), and **(C)** at 4 weeks (after isoproterenol perfusion). Results are presented as mean ± SEM. Global p-value shown was obtained by nonparametric Kruskal-Wallis and the p-value among different treatments was determined by nonparametric 1-way ANOVA after Dunn's post hoc test.

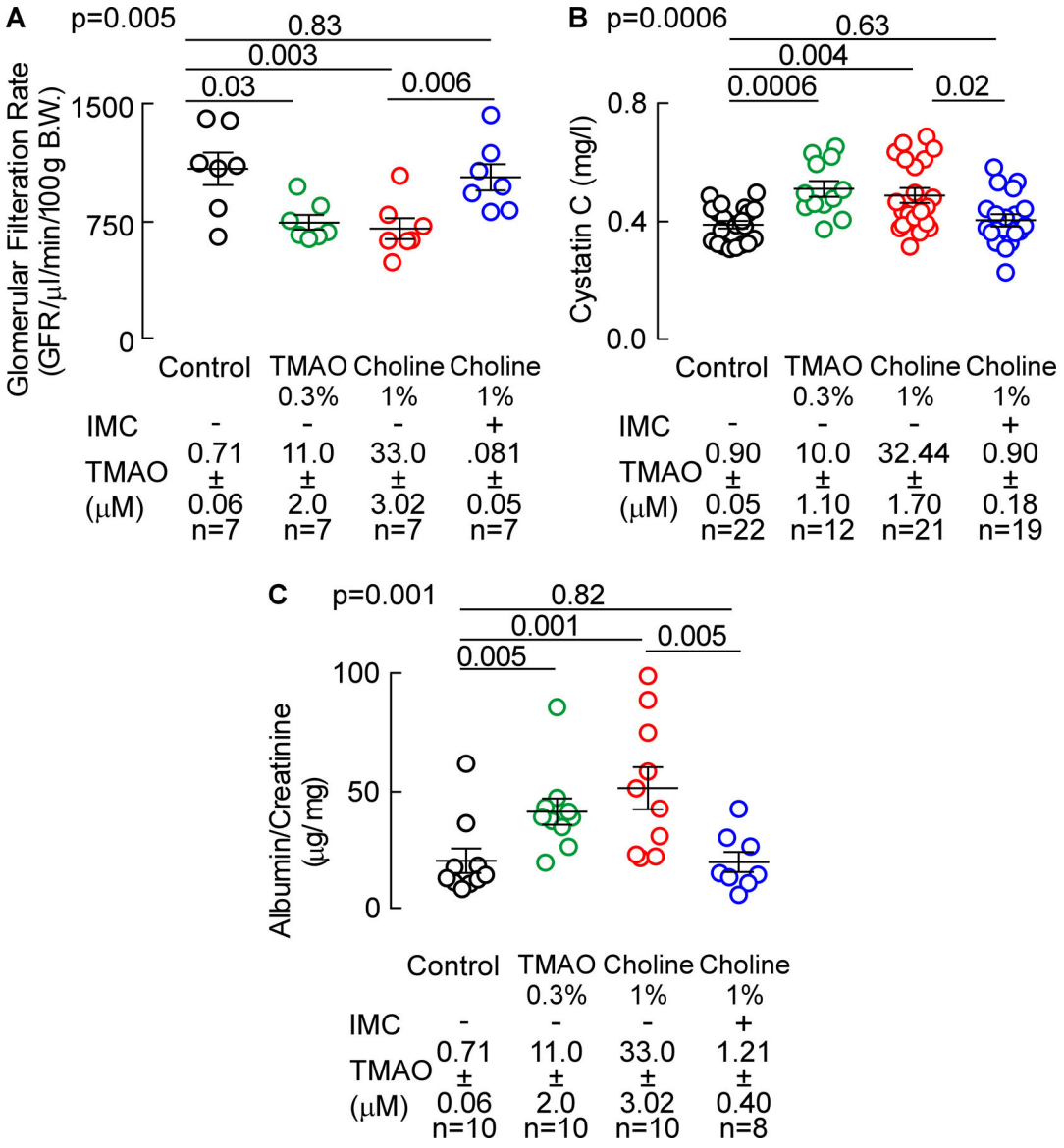

Figure 4. Microbial choline TMA-lyase inhibitor IMC attenuates choline diet-induced renal functional impairment.

(A) Glomerular filtration rate **(GFR), (B)** plasma Cystatin C, and **(C)** urinary albumin to creatinine ratio (ACR). Results are presented as mean ± SEM. Global p-value shown was obtained by nonparametric Kruskal-Wallis and the p-value among different treatments was determined by nonparametric 1-way ANOVA after Dunn's post hoc test.

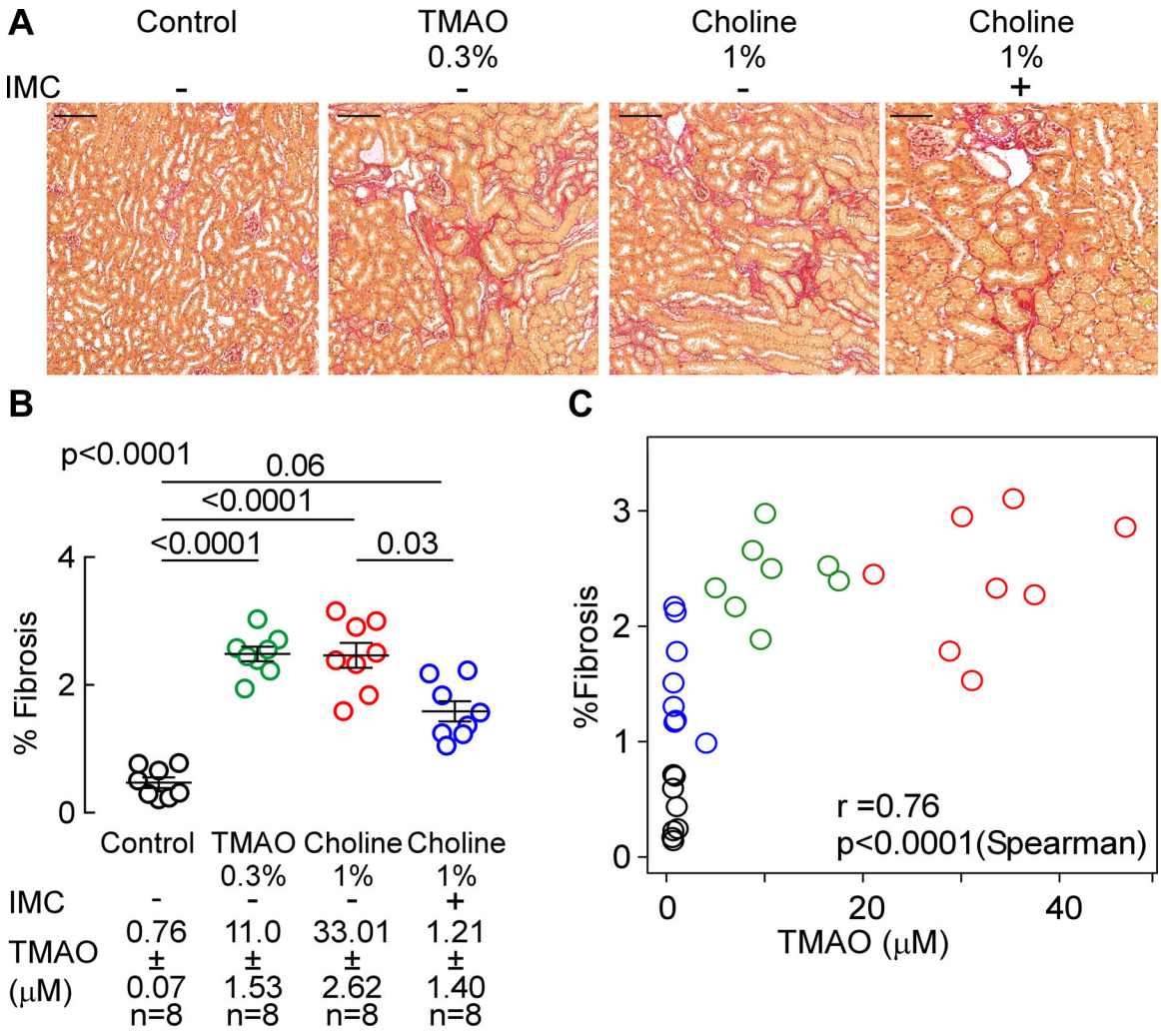

Figure 5. Microbial choline TMA-lyase inhibitor IMC attenuates choline diet-induced renal tubulointerstitial fibrosis.

(A) Representative photomicrographs of picrosirius red-stained kidney (scalebar=100 microns), **(B)** fibrosis quantification, and **(C)** correlation between plasma TMAO and %fibrosis. Results are presented as mean ± SEM. Global p-value shown was obtained by 1-way ANOVA (Kruskal-Wallis) and the p-value among the different treatments was determined by 1-way ANOVA (Kruskal-Wallis) after Dunn's post hoc test and spearman correlation.

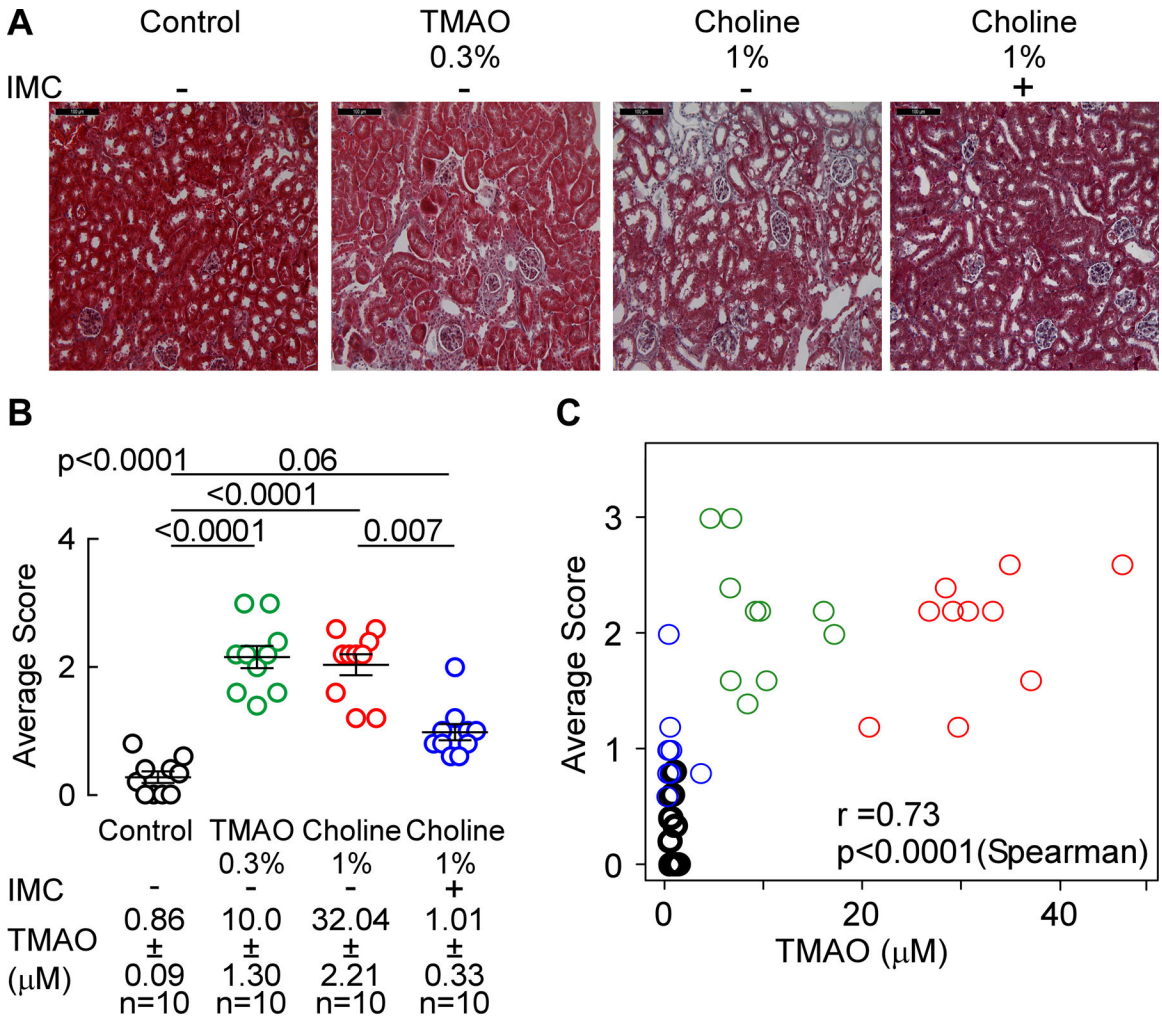

Figure 6. Microbial choline TMA-lyase inhibitor IMC attenuates choline diet-induced renal tubulointerstitial fibrosis.

(A) Representative photomicrographs of Masson's trichrome-stained (scalebar=100 microns), **(B)** histological scoring of Masson's trichrome stained kidneys, and **(C)** correlation between renal histological score and plasma TMAO. Mean scores per mouse ± SEM are shown and global p-value was obtained by 1-way ANOVA (Kruskal-Wallis) and the p-value among the different treatments was determined by 1-way ANOVA (Kruskal-Wallis) after Dunn's post hoc test and Spearman's correlation.

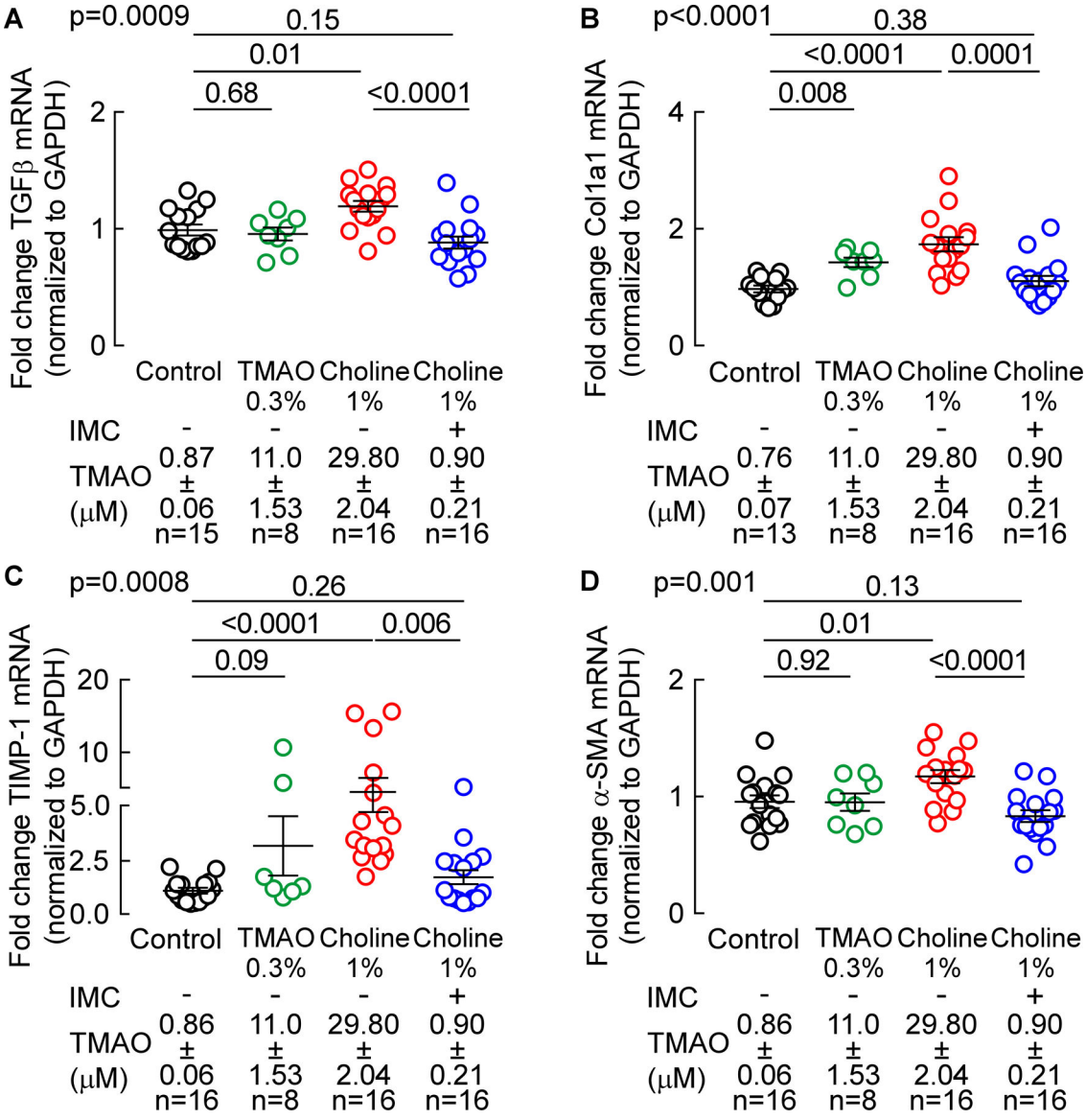

Figure 7. Microbial choline TMA-lyase inhibitor IMC attenuates choline diet-induced renal profibrotic gene expression changes.

Profibrotic gene expression, normalized to GAPDH mRNA transcripts, in murine kidney was analyzed by TaqMan real-time polymerase chain reaction. **(A)** Transforming growth factor - b (TGF-b), **(B)** a-1- type1 collagen (Col1a1), **(C)** TIMP-1 gene expression, and **(D)** a-SMA (smooth muscle actin). Results are presented as mean ± SEM. Global p-value shown was obtained by nonparametric Kruskal-Wallis and the p-value among different treatments was determined by nonparametric 1-way ANOVA after Dunn's post hoc test.

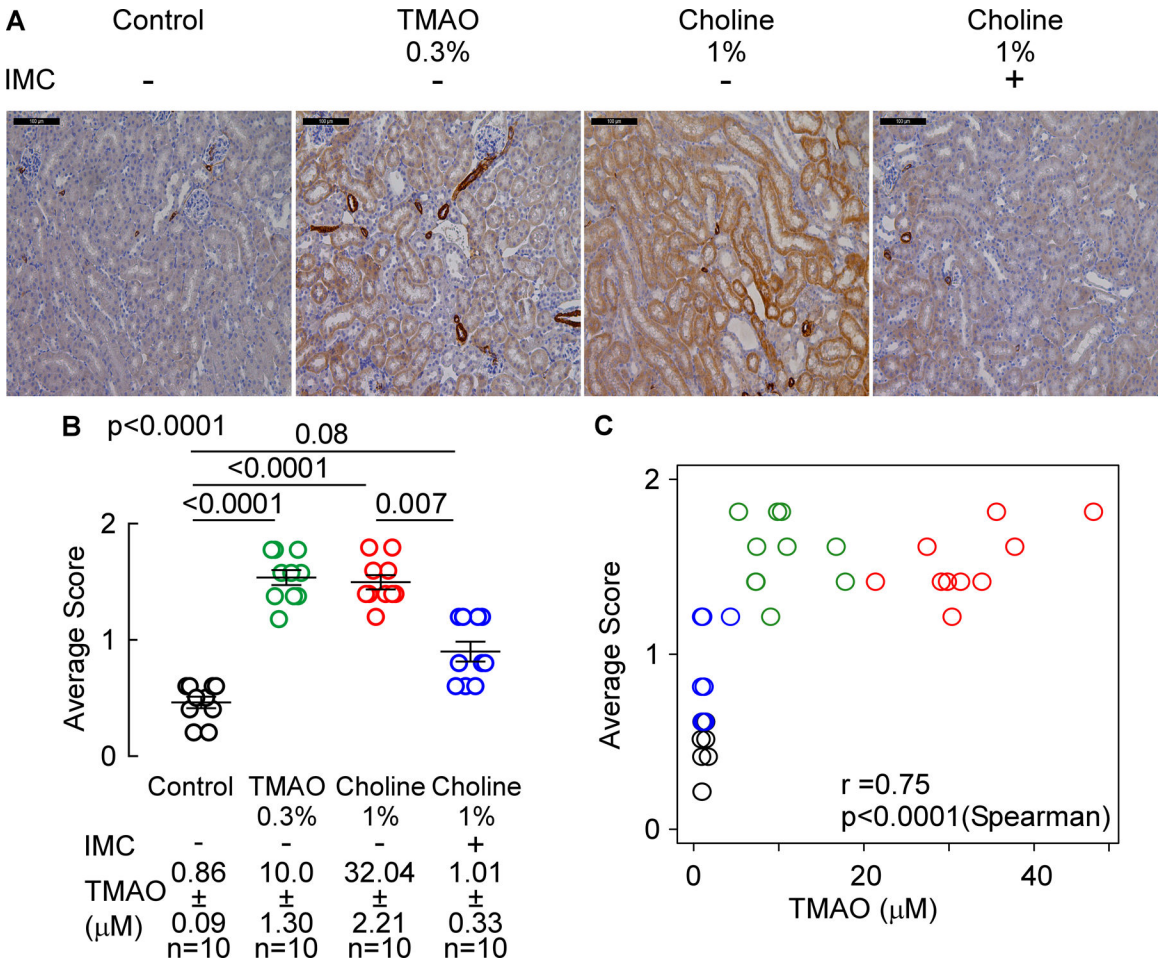

Figure 8. Microbial choline TMA-lyase inhibitor IMC attenuates choline diet-induced alpha-smooth muscle actin protein expression.

(A) Representative a-SMA renal immunohistochemistry pictographs (scalebar= 100 microns), **(B)** a-SMA protein levels score, and **(C)** plasma TMAO levels correlation with prevalence of a-SMA staining. Results are presented as mean ± SEM. Global p-value shown was obtained by nonparametric Kruskal-Wallis and the p-value among different treatments was determined by nonparametric 1-way Anova after Dunn's post hoc test. For correlation between plasma TMAO levels and a-SMA staining, p-values were calculated using nonparametric Spearman's correlation.

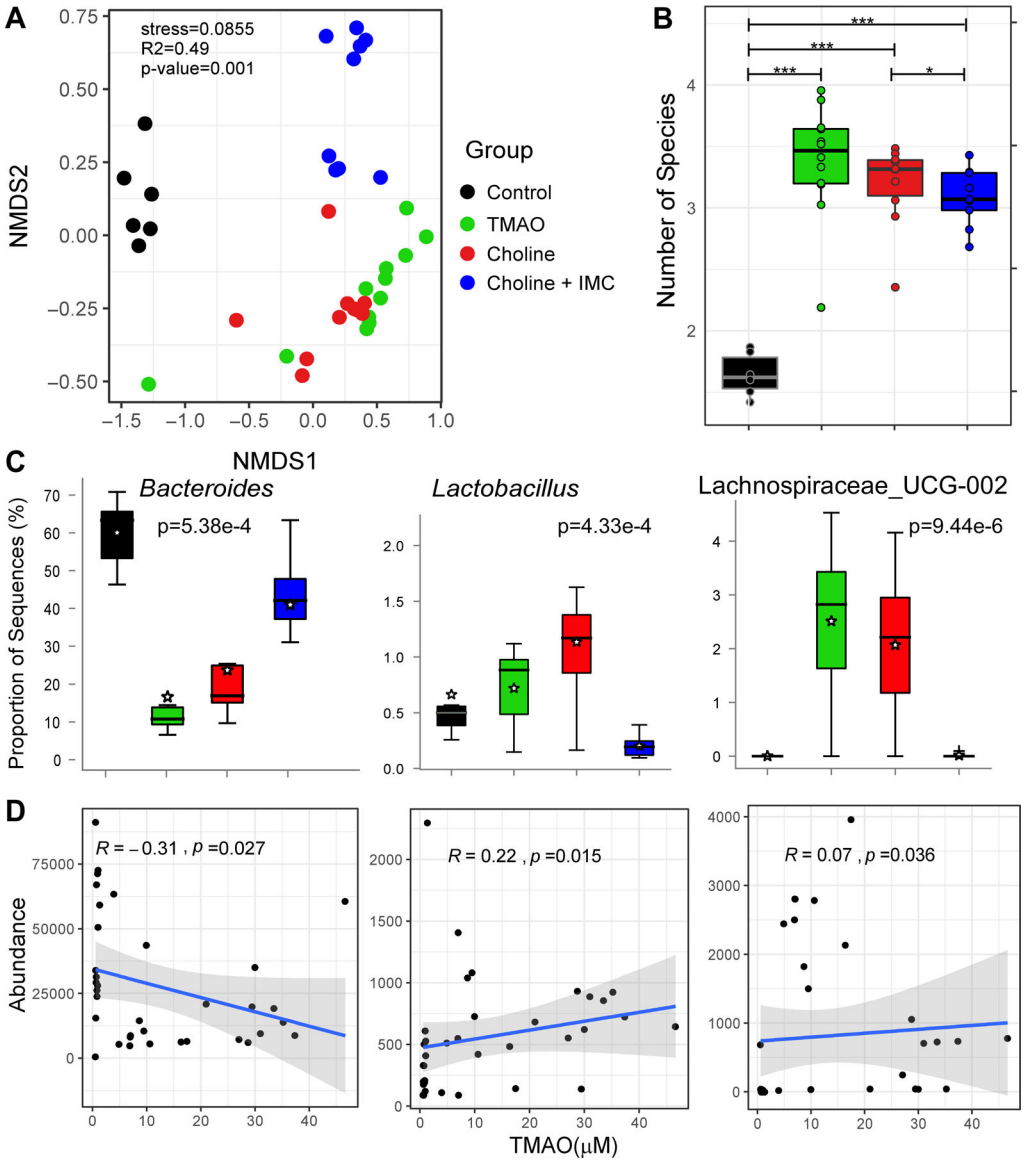

Figure 9. TMA-lyase inhibitor, IMC, impacts the choline diet-induced changes in cecal microbial community associated with plasma TMAO levels.

(A) The non-metric multidimensional scaling plots (NMDS) based on Bray Curtis index between the cecal microbiota of mice treated with indicated diets i.e. Control, TMAO, Choline, and Choline + IMC samples. Each data point represents a sample from a distinct mouse. Statistical analysis was performed using PERMANOVA and p-values are labelled in the plots. R2 values are also mentioned for comparisons with significant p-values. The R2 values stand for % variance explained by the variable of interest i.e. diet. **(B)** Boxplots of Shannon diversity indices distinguishing Control, TMAO, Choline, and Choline + IMC samples. Statistical analysis was performed using paired t-tests. Plotted are interquartile ranges (boxes) and the dark line in the box is the median. *** stands for p-value<=0.001 and * stands for p-value <0.05. **(C)** Multi-group Kruskal-Wallis H-test showing results for statistically significant (BH-FDR p < 0.05) genera differentiating four groups i.e. Control, TMAO, Choline, and Choline + IMC. **(D)** Linear regression based scatter plots showing

correlation between abundance of select taxa and TMAO (μM) levels. The R2 and p-values are plotted within each panel.